Chapter 20

# Linear-elastic response of starch-based materials: FFT results vs. experimental data

François Willot[1] & Sofiane Guessasma[2]

[1] Mines ParisTech, PSL – Research University, Centre for Mathematical Morphology, 35 rue Saint-Honoré, 77300 Fontainebleau, France,
[2] INRA, Unité de recherche sur les Biopolymères, Interactions & Assemblages, rue de la Gérausière, 44316 Nantes, France

**Keywords:** Fourier methods; Biopolymer; Starch

**Abstract** Comparisons are made between Fourier-based numerical computations and experimental measurements for Young's moduli of a biopolymeric foam material with high porosity. The effect of grid resolution and the representativity of the 3D images are investigated.

## 20.1 Starch-based foam material

This work is concerned by two sets of biological materials with open-foam structures, as shown in Fig. (20.1). Set A is represented by 8 samples with relative (volumetric) density ranging from 0.08 to 0.19 and set B by 4 samples with relative densities in-between 19 and 33%. Experimental measurements are carried out for the macroscopic measurement of Young's moduli of each foam, as well as for Young's modulus of the cell walls in the foam. Each sample is characterized by a segmented 3D image, containing a portion of the original material, with volume ranging from $50^3$ to $480^3$ voxels.

## 20.2 Fourier computations

The numerical FFT method (Michel, Moulinec, and Suquet 2000) is applied to each segmented images. Small deformation are assumed and the local behavior of starch is approximated by an isotropic, incompressible linear elastic law. Incompressibility is approached by setting $K = 10^3$ (a.u.) for the bulk modulus in the walls, $G = 1$ (a.u.) for the shear modulus, and vanishing elastic moduli in the pores. An example of an FFT map for the stress field is shown in Fig. (20.2), as well 2D sections of the deformed and undeformed material. As expected, the material behavior is found to be macroscopically compressible due to the presence of voids, and according to the numerical computations, roughly isotropic. In addition, stress heterogeneity develops as a result of the stress concentrators reflected by the presence of the porous network.

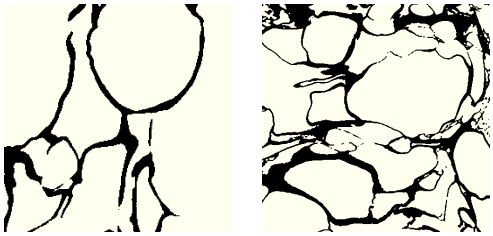

(a) (b)

Figure 20.1: Segmented images of starch-based materials. Black: starch. White: porosity. Two samples from sets A (a) and B (b) are shown, as 2D sections. The image resolutions are $260^3$ (a) and $430^3$ voxels (b), and the porosity is 79% (a) and 92% (b) in the two samples.

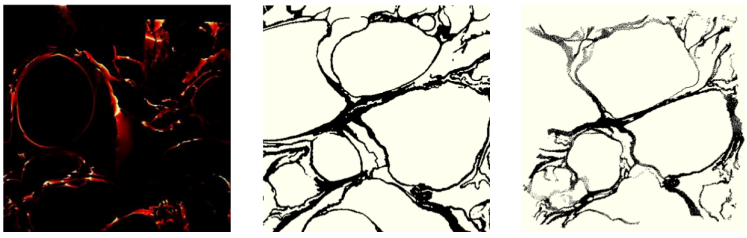

(a) (b) (c)

Figure 20.2: Linear elastic behavior of starch composites, as computed by the FFT numerical method: (a) map of the mean stress field $\sigma_m$, cut along a plane (stress is null in black regions, and high in red/white zones), (b) microstructure with starch in black and voids in white, (c) magnified microstructure evolution at first-order. A hydrostatic strain loading $\langle \varepsilon_m \rangle = \varepsilon_0$ with $\varepsilon_0 = 10\%$ is applied.

We first examine the effect of image resolution on the apparent elastic properties. Sample images are discretized on coarse grids containing $L^3$ voxels (varying $L$) as represented in Fig. (20.3). The apparent Young's modulus is represented as a function of the number of voxels in the grid along a given direction, $L$, where $L$ monitors the image resolution (Fig. 20.4a). As seen in this plot, the apparent moduli converge to a limiting value for most of the samples.

Second, we investigate the representativity of the samples (Fig. 20.4b). To this end, a sample of set A of size $460^3$ is subdivided into non-interpenetrating subvolumes of increasing sizes $L^3 = 100^3$ up to $L^3 = 240^3$ voxels. Fourier computations are carried out on each subdomain. The dispersion of the apparent Young's modulus is determined using standard deviation and min/max values. As expected, the median and mean of Young's modulus converge to a limiting value for large subdomains. This data suggest a relative precision of less than 15%.

## 20.3 FFT computations vs. experimental results

The homogenized Young's modulus $E_0$ is computed using the FFT method for each sample of each set. Young's modulus is normalized by the wall's Young modulus $E$. Figure (20.5) shows Fourier predictions for the normalized effective modulus $E_0/E$ vs. the foam macroscopic relative density $f$ (symbols in-between solid lines). These results are compared to experimental data (symbols in-between dashed lines), for both sets.

The behaviors of the Young moduli vs. foam density in the two sets A and B are notably different, with set B's mechanical response more compliant than set A's. As


Figure 20.3: Same microsrtucture, discretized on grids of $L^3 = 50^3$ (a), $100^3$ (b) and $200^3$ voxels (c).

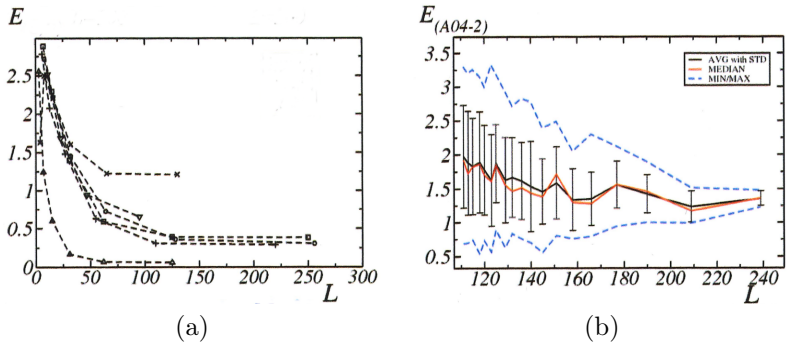


Figure 20.4: (a) *Effect of grid resolution.* Apparent Young's modulus (a.u.) predicted by Fourier methods vs. number of voxels $L^3$ used to discretize the foam structure, for various samples in sets A and B. (b) *Representativity.* Apparent Young's modulus (a.u.) computed by applying the Fourier method to subvolumes extracted from a sample in set A, represented as a function of the subvolume size $L$. Black: mean values (error bars are standard deviations). Orange: median. Blue dashed lines: minimum and maximum apparent modulus.

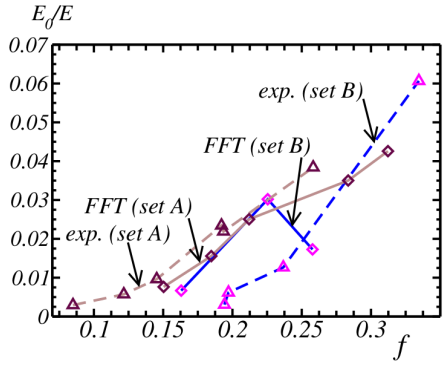


Figure 20.5: Normalized macroscopic Young modulus $E_0/E$ as a function of the density $f$: comparison between FFT results and experimental data, for two sets (A) and (B) of microstructures.

expected, the normalized effective moduli for sets A and B lie very much beneath the corresponding Hashin-Shtrikman upper-bounds, and are are somewhat more compliant than Ashby's law $E_0/E \approx f^2$ (Ashby 2006) (not shown).

Note that the relative density in the experimental data differs from that used in the FFT computations. This is because the 3D images of the materials, to which we apply the FFT method, are only a small part of each sample. Nevertheless, for set A, the apparent moduli predicted by FFT as a function of the relative density are close to experimental data. The same result holds for set B, with the exception of one aberrant FFT point which lies significantly outside the experimental data.

## 20.4 Conclusion

The elastic response of starch-based materials has been predicted by Fourier numerical computations based on 3D segmented images. Two sets of foam structures were considered with several samples in each set. The foam structures display a large porosity content (up to 90%), which needs to be voxelized when using FFT methods. Despite this, Fourier-based computations were able to predict the macroscopic Young's moduli vs. foam density, qualitatively and, with an acceptable precision, quantitatively.

**Acknowledgements** The authors are grateful to Guy Della Valle & Anne-Laure Reguerre (INRA, Nantes) for providing microstrure images and experimental data, and to Dominique Jeulin for useful discussions and for organizing the Mécamat Workshop *Journées Thématiques des Groupes de Travail: Approches Probabilistes en Mécanique des Milieux Hétérogènes – Rhéologie des Matériaux Hétérogènes – Traitements Thermomécaniques* in Bordeaux, France, May 14–15, 2009.

### References

Ashby, MF (2006). "The properties of foams and lattices". In: *Philosophical Transactions of the Royal Society of London A: Mathematical, Physical and Engineering Sciences* 364.1838, pp. 15–30.

Michel, J.-C., H. Moulinec, and P. Suquet (2000). "A computational method based on Augmented Lagrangians and Fast Fourier Transforms for composites with high contrast". In: *Computer Modelling in Engineering & Sciences* 1.2, pp. 79–88.